An Overshoot Algorithm for Filament Winding of Circular Cylinders

J.M. Dolan, P.K. Khosla, and S.N. Talukdar

1.0 Problem Overview

Helical filament-winding is performed by dispensing filament through a filament delivery point onto a rotating mandrel. The longitudinal length traversed by the winding point on the mandrel is inevitably smaller than the longitudinal distance traversed by the delivery point, due to the nature of the differential equation of winding. However, since it is simple to set the delivery point traverse to the desired winding point traverse, the typical solution is to introduce pauses in the delivery point motion at the desired filament layer endpoints in order to allow the filament position to exponentially approach its desired value. A preferable solution which reduces time and material is to have the delivery point overshoot the desired winding point endpoints by the amount necessary to ensure that the filament exactly reaches the the desired endpoints. For a conventional winding machine having only three settings, i.e., the delivery point traverse, endpoint pause, and pitch (or equivalently, the winding angle), the problem involves simultaneously achieving: 1) the desired winding-point traverse, and 2) the correct band-center shift along the mandrel perimeter to ensure pattern closure. This report presents a method for meeting these two conditions.

2.0 Problem Solution

The overshoot algorithm simultaneously fulfills two conditions on the delivery point traverse L' and the mandrel rotation pause value n'_{ψ}. The prime notation is used to distinguish the overshoot traverse and pause from the conventional, non-overshoot traverse and pause, L and n_{ψ}. Section 2.1 derives the endpoint condition, which ensures that the desired winding point traverse L is achieved. Section 2.2 presents the band-shift condition, which ensures that bands in successive passes are propertly shifted with respect to one another so as to ensure closure. Section 2.3 presents a solution for simultaneous fulfillment of these two conditions.

2.1 Endpoint Condition

The differential equation relating the longitudinal motion of the winding-point x to that of the filament delivery point X for a circular cylinder is [1]:

$$\dot{x} = \frac{v_0}{l}(X - x) \tag{EQ 1}$$

where $v_0 = \omega r$, where ω is the rotational velocity of the mandrel and r is its radius, and l is the length of the filament from winding-point to delivery point perpendicular to the mandrel's axis of rotation. By introducing the notation

$$p \equiv \frac{v_0}{l}$$

we can write

$$\dot{x} = p(X - x) \qquad \text{(EQ 2)}$$

A general solution of this equation taking into account the cyclical nature of the delivery point $X(t)$ was presented by Efremov [1]. An approximation of the conventional delivery point motion $X(t)$ is depicted in Figure 1. The delivery point traverse is L', the pause time at each end of the delivery point trajectory is η seconds, and the traverse time from one end to the other is τ seconds. The corresponding longitudinal winding point traverse is L. The delivery point velocity during traversal of the mandrel is denoted by V.

FIGURE 1. Conventional Delivery Point Motion

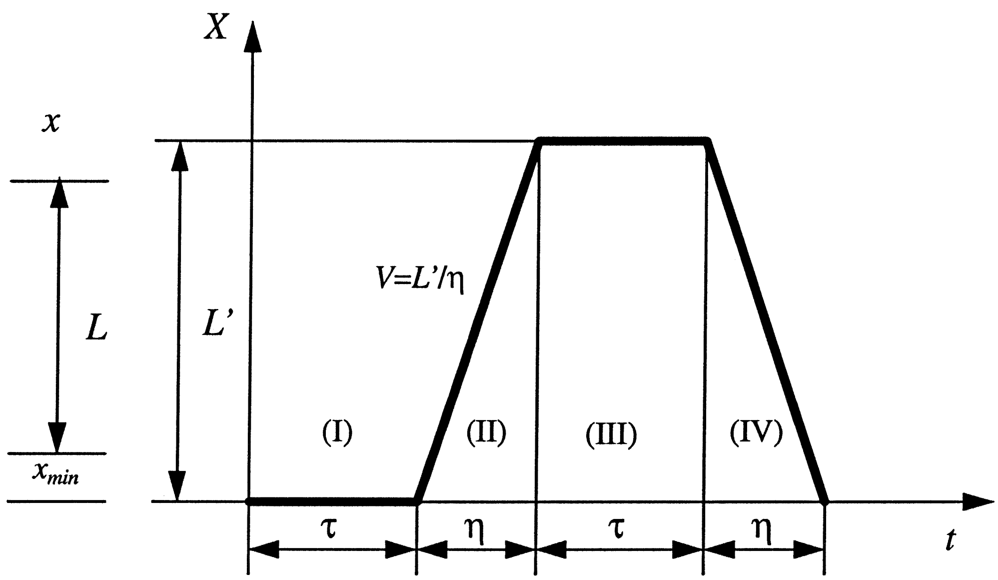

Solving (2) by the method presented in [1] with $X(t)$ as depicted in Figure 1, we obtain

$$x_{(I)} = \frac{V}{p} Q e^{-p(t-\tau)} \qquad 0 \le t \le \tau$$

$$x_{(II)} = V(t-\tau) - \frac{V}{p}\left(1 - (1+Q)\, e^{-p(t-\tau)}\right) \qquad \tau \le t \le \tau + \eta$$

$$x_{(III)} = L' - \frac{V}{p} Q e^{-p(t-2\tau-\eta)} \qquad \tau + \eta \le t \le 2\tau + \eta$$

$$x_{(IV)} = -V(t - 2\tau - 2\eta) + \frac{V}{p}\left(1 - (1+Q)\, e^{-p(t-2\tau-\eta)}\right) \qquad 2\tau + \eta \le t \le 2\tau + 2\eta$$

where

$$Q \equiv \frac{e^{p\eta} - 1}{e^{p(\tau+\eta)} + 1} \qquad\qquad 1 + Q = \frac{e^{p\eta}(e^{p\tau} + 1)}{e^{p(\tau+\eta)} + 1}$$

If the desired winding point traverse is L and the delivery point traverse $L' = L$, then the desired winding point traverse will never be attained. At each L' larger than L, however, a certain pause value τ results in the desired winding point traverse L. We therefore seek a relationship between L' and τ, or equivalently, between L' and n'_{ψ}, the number of mandrel pause turns per pass. The relationship between n'_{ψ} and τ is

$$2\tau = \left(\frac{2\pi}{\omega}\right) n'_{\psi}$$

We note first that the extreme values of $x(t)$ occur in regions (II) and (IV), when the delivery point is traversing the mandrel. This can be seen by considering that the value of x must continue to move in the same direction for some time after a pause, since at the end of a pause, the delivery point position lies beyond the current value of x. Thus, in order to find the time t_{min} at which the winding point reaches its minimum value x_{min}, the derivative with respect to t of $x(t)$ in region (II) is set to zero:

$$\frac{dx}{dt}_{(\mathrm{II})} = V - V(1+Q)\,e^{-p(t-\tau)} = 0 \qquad \text{(EQ 3)}$$

Solving this equation for t, we obtain

$$t_{min} = \tau + \frac{1}{p}\ln(1+Q) \qquad \text{(EQ 4)}$$

Equation (4) is now substituted into the expression for $x_{(\mathrm{II})}$ in order to find x_{min}:

$$x_{min} = \frac{V}{p}\ln(1+Q) \qquad \text{(EQ 5)}$$

The delivery point traverse is symmetric about the winding point traverse, so we can write

$$\frac{L' - L}{2} = x_{min} = \frac{V}{p}\ln(1+Q) \qquad \text{(EQ 6)}$$

Multiplying (6) through by p/V and raising both sides to a power of e, we obtain

$$e^{\frac{p(L'-L)}{2V}} = 1 + Q = \frac{e^{p\eta}(e^{p\tau} + 1)}{e^{p(\tau+\eta)} + 1} \qquad \text{(EQ 7)}$$

Seeking to isolate τ, we define

$$\alpha \equiv \frac{p(L' - L)}{2V} \qquad \text{(EQ 8)}$$

and multiply (7) through by the denominator of the right-hand side

$$e^{\alpha}(e^{p(\tau+\eta)} + 1) = e^{p(\tau+\eta)} + e^{p\eta} \qquad \text{(EQ 9)}$$

Bringing all the terms not in τ to the right-hand side yields

$$e^{p\tau} = \frac{e^{p\eta} - e^{\alpha}}{e^{p\eta}(e^{\alpha} - 1)} = \frac{1 - e^{\alpha - p\eta}}{e^{\alpha} - 1} \qquad \text{(EQ 10)}$$

Taking the natural logarithm of both sides of (10), we obtain

$$\tau = \frac{1}{p}\ln\left(\frac{1 - e^{\alpha - p\eta}}{e^{\alpha} - 1}\right) \qquad \text{(EQ 11)}$$

We now perform several transformations in order to put (11) into more familiar terms. First, note that

$$\frac{V}{p} = V\left(\frac{l}{v_0}\right) = l\left(\frac{V}{v_0}\right) = l\tan\theta_f \qquad \text{(EQ 12)}$$

where θ_f is the filament winding angle measured from the perpendicular to the axis of rotation. This proceeds from the fact that the ratio of the delivery point velocity to the tangential winding point velocity is equal to the tangent of the winding angle. Equations (8) and (12) lead to

$$\alpha = \frac{L' - L}{2l\tan\theta_f} \qquad \text{(EQ 13)}$$

The exponential argument $p\eta$ may also be rewritten:

$$p\eta = \left(\frac{v_0}{l}\right)\left(\frac{L'}{V}\right) = \left(\frac{v_0}{l}\right)\left(\frac{L'}{v_0\tan\theta_f}\right) = \frac{L'}{l\tan\theta_f} \qquad \text{(EQ 14)}$$

Finally, by noting that

$$p\tau = \left(\frac{v_0}{l}\right)\left(\frac{\pi n'_{\psi}}{\omega}\right) = \frac{\pi r n'_{\psi}}{l} \qquad \text{(EQ 15)}$$

and substituting (13)-(15) into (11), we obtain

$$n'_{\psi} = \frac{l}{\pi r}\ln\left(\frac{1 - e^{\frac{-(L'+L)}{2l\tan\theta_f}}}{e^{\frac{L'-L}{2l\tan\theta_f}} - 1}\right) \quad \text{(EQ 16)}$$

Given values for the delivery point standoff l, the winding angle θ_f, the mandrel radius r, and the desired winding point traverse L, Equation (16) gives the relationship between the delivery point traverse L' and the number of mandrel pause turns n'_{ψ}.

2.2 Band-Shift Condition

The endpoint condition taken alone implies that L' and n'_{ψ} can take on a continuum of values as long as $L' > L$. However, it is additionally necessary to ensure that the band-shift at a given cross-section is such that the repetitive pattern produced by the delivery point motion shown in Figure 1 results in closure. The closure algorithm is summarized here from [2]:

1. Find the number of bands

$$Bz = \frac{2\pi r\tan\theta_f}{B} \quad \text{(EQ 17)}$$

where B is the filament band width, and θ_f has been adjusted to ensure that Bz is an integer.

2. Find the per-pass band-center-position shift in mandrel turns

$$n_{\phi} = \frac{L}{\pi r\tan\theta_f} \quad \text{(EQ 18)}$$

3. Find the set of integer multiples $\{j_s\}$ of $\frac{1}{Bz}$ which produce the fractional parts, n_f, of valid solutions for the number of mandrel turns per pass, n. The j_s consist of all j, $0 < j < m$, such that j and m are relatively prime, i.e., they have no common factor greater than 1.

4. Find valid solutions $n \geq n_{\phi}$ having allowable fractional parts

$$\{n_f\} = \frac{\{j_s\}}{m} \quad \text{(EQ 19)}$$

The result of (17)-(19) is a set of valid solutions for n, the total number of mandrel turns per pass. The band-shift condition is given by

$$n = n'_{\phi} + n'_{\psi} = \frac{L'}{\pi r\tan\theta_f} + n'_{\psi} \quad \text{(EQ 20)}$$

By specifying the left-hand side of (20) with one of the valid solutions for n found in (17)-(19), a second continuous relationship between the delivery point traverse L' and the number of mandrel pause turns n'_{ψ} is established.

2.3 Simultaneous Satisfaction of Endpoint and Band-Shift Conditions

A solution for L' and n'_ψ which satisfies both (16) and (20) must now be found. Substitution of (16) into (20) yields

$$n = \frac{L'}{\pi r \tan\theta_f} + \frac{l}{\pi r}\ln\left(\frac{1 - e^{\frac{-(L'+L)}{2l\tan\theta_f}}}{e^{\frac{L'-L}{2\tan\theta_f}} - 1}\right) \tag{EQ 21}$$

Multiplying through by $\pi r/l$, moving terms, and raising both sides to powers of e, we obtain

$$e^{\frac{\pi r n}{l}} e^{-\frac{L'}{l\tan\theta_f}} = \frac{1 - e^{\frac{-(L'+L)}{2l\tan\theta_f}}}{e^{\frac{L'-L}{2l\tan\theta_f}} - 1} \tag{EQ 22}$$

By defining

$$\gamma \equiv \frac{\pi r n}{l} \tag{EQ 23}$$

$$\delta \equiv \frac{1}{2l\tan\theta_f} \tag{EQ 24}$$

we can rewrite (22) as

$$e^{\gamma} e^{-2\delta L'} = \frac{1 - e^{-\delta(L'+L)}}{e^{\delta(L'-L)} - 1} \tag{EQ 25}$$

Simplification of (25) yields

$$e^{2\delta L'} - e^{-\delta L}(e^{\gamma} + 1)e^{\delta L'} + e^{\gamma} = 0 \tag{EQ 26}$$

Equation (26) can be written in the form of the following quadratic equation

$$x^2 + bx + c = 0 \tag{EQ 27}$$

where

$$x \equiv e^{\delta L'} \tag{EQ 28}$$

$$b \equiv -e^{-\delta L}(e^{\gamma} + 1) \tag{EQ 29}$$

$$c \equiv e^{\gamma} \tag{EQ 30}$$

The solutions to (27) are

$$x = \frac{-b \pm \sqrt{b^2 - 4c}}{2} \qquad \text{(EQ 31)}$$

However, only the solution

$$x = \frac{-b - \sqrt{b^2 - 4c}}{2} \qquad \text{(EQ 32)}$$

leads to non-negative values for n'_ψ. Once x is found from (32), *L'* may be determined from (28):

$$L' = \frac{1}{\delta}\ln(x) \qquad \text{(EQ 33)}$$

The corresponding value of n'_ψ is found by inserting the solution for *L'* found in (32) into (20).

3.0 Example and Notes on Implementation

For purposes of illustration, we choose a mandrel with diameter $D = 400$ mm and length $L = 1000$ *mm*, band width $B = 40$ *mm*, delivery point standoff $l = 150$ *mm*, and a desired winding angle $\theta_f = 30°$. Applying the closure algorithm, we obtain the solution set for n and n_ψ shown in Table 1.

TABLE 1. Conventional Closure Solutions for n and n_ψ with D=400, L=1000, l=150 *mm*

n, turns	n_ψ, turns
2.9444	0.1667
3.0556	0.2778
3.2778	0.5000
3.3889	0.6111
3.7222	0.9444
3.9444	1.1667

The last solution, $n = 3.9444$, $n_\psi = 1.1667$, is the one chosen by the algorithm implemented at ABB Brilon in July, 1992. It is the solution having the smallest pause value in the range $n_\psi = 1.1$ to 1.3.

The overshoot algorithm is now applied to each of the solutions for n given in Table 1. The results are shown in Table 2. For the two smallest pause values, there is no feasible solution. This shows itself mathematically in a negative quantity under the square root in (32). The third valid value for n has a solution with an overshoot of 26.7 *mm* (13.35 *mm* on each end of the mandrel). For a given value for n, the overshoot pause value n'_ψ is smaller than its corresponding conventional pause value n_ψ. This is because traversal of the overshoot length L' takes longer than traversal of the conventional length L, and a given value for n'_ϕ is thus greater than its corresponding n_ϕ. As n increases, the overshoot length decreases, and the overshoot and conventional pause values approach one another.

TABLE 2. Overshoot Closure Solutions for the *n* given in Table 1

n, turns	*L'*, *mm*	n'_ψ, turns	% Savings
2.9444	---------No solution---------		-------
3.0556	---------No solution---------		-------
3.2778	1026.7	0.4258	16.9
3.3889	1015.2	0.5690	14.1
3.6111	1005.5	0.8180	8.4
3.7222	1003.4	0.9350	5.6
3.9444	1001.3	1.1630	0.0

FIGURE 2. Graphical Representation of Satisfaction of Endpoint and Band-Shift Conditions

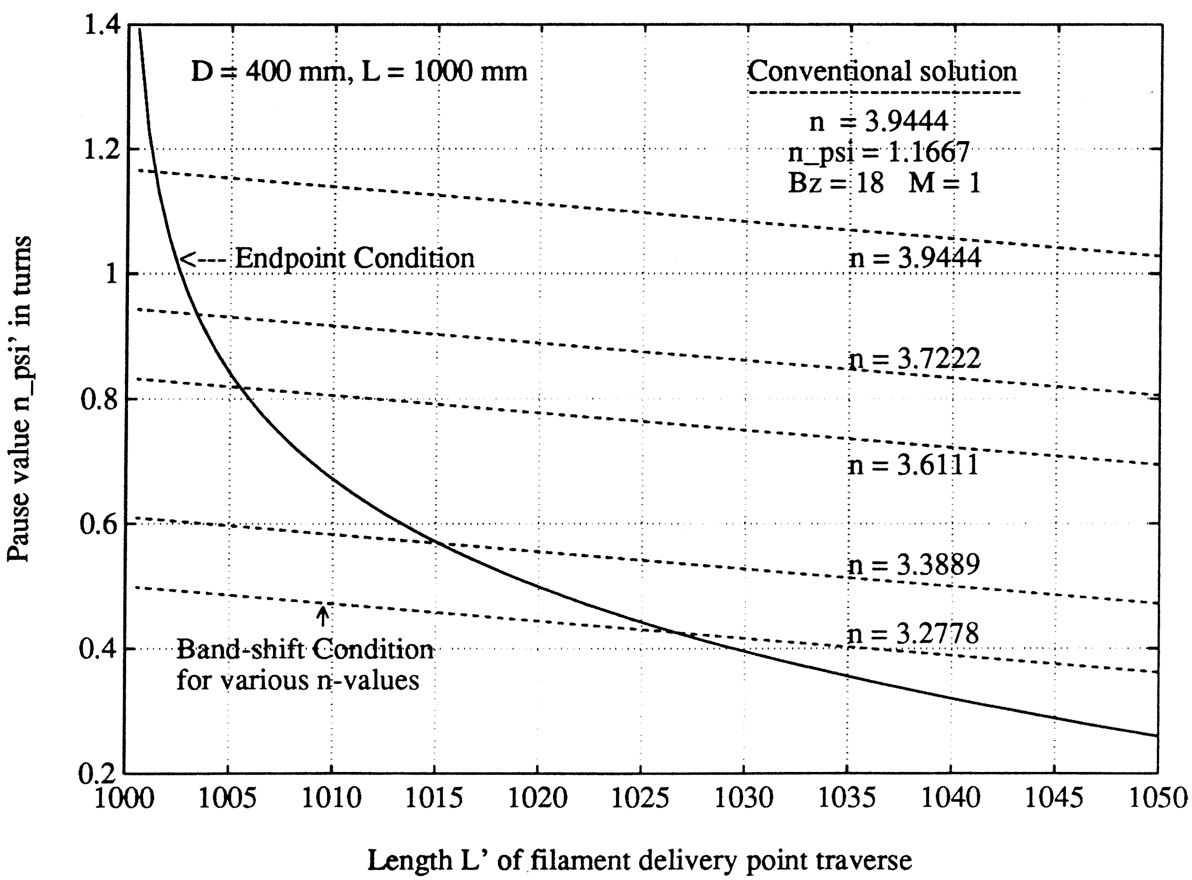

Figure 2 graphically depicts the simultaneous satisfaction of the endpoint and band-shift conditions for the current example. The exponentially decreasing curve represents the endpoint condition, while the dotted straight lines represent the band-shift condition for various values of n. For a given value of n, the point of intersection of the endpoint and band-shift curves represents the solution for L' and n'_{ψ}. The software provided with this report prints out Table 2 after receiving L, D, and l as inputs. The band width and desired winding angle are set as global variables, but they can also be adjusted.

Given a table of overshoot solutions such as Table 2, the overshoot algorithm may be tested on the winding machines currently in use. The winding machines require three settings: delivery point traverse L', pause value n'_{ψ}, and pitch $h = 2\pi r \tan\theta_f$. The first two are provided by the overshoot algorithm, and the pitch remains the same for both the conventional and overshoot algorithms. In order to use the overshoot algorithm, the delivery point standoff l must be measured, and the delivery point traverse L' must be settable with a sufficiently fine resolution. If these two things can be done, the solutions given in Table 2 may be tested, starting with the n-value corresponding to the conventional solution, and decreasing n until band slippage occurs. In the current example, if slippage does not occur, there is a potential for a 16.9% savings in time and material for the helically wound layers with respect to the conventional solution. It may be possible to analytically predict at which n-value slippage will begin based on the rate of change of the winding angle in the end regions and the friction properties of the resin. This is an area for further work.

References

1. Efremov, E.D., Movement of the Winding Point along the Generator of a Cylindrical Bobbin, *Tech. of the Textile Industry U.S.S.R.*, pp. 90-102, 1962.

2. Dolan, J.M., Gatenholm, M., Khosla, P.K., Talukdar, S.N., Filament Winding Algorithms for Arbitrary Convex Mandrel Shapes, *Technical Report submitted to ABB Brilon*, pp. 15-18, July 9, 1992.